Numerical Verification of the Dispersion Relation of Trapezoidally Corrugated Slow Wave Structure for Backward Wave Oscillators

Md. Rasheduzzaman Al-Amin [1*], Md. Ruhul Amin [1], Rakibul Hasan Sagor[1]

[1] Department of Electrical and Electronic Engineering, Islamic University of Technology, Board Bazar, Gazipur-1704, Bangladesh.
[*]rasheduzzaman@iut-dhaka.edu

Abstract: The dispersion relation of beam free trapezoidally corrugated periodic metallic slow wave structure (TCSWS) has been numerically verified using synthetic technique. The dispersion curves for both the fundamental and the higher order passband modes (TM_{01} – TM_{03}) are computed for the axisymmetric corrugated structure. The periodic structure resonates at specific frequencies when shorted appropriately at both ends. From the specific frequency values of these resonant peaks, dispersion curve is determined for each TM modes. The obtained dispersion curve is compared with both the experimental and analytical results using same number of periods. The comparisons with analytical results and their experimental counterpart agree excellently with a maximum deviation of 1.94% for TM_{01} mode, 1.29% for TM_{02} mode and 2.38% for TM_{03} mode. The radial and longitudinal electromagnetic field patterns of TCSWS are also calculated and compared with analytical field patterns for a six-period slow wave structure (SWS). Comparative results validate both the obtained dispersion curves and field patterns of TCSWS.

1. Introduction

Backward wave oscillators (BWOs) are the typical examples of slow wave type high power microwave (HPM) devices that generates hundreds of megawatts to gigawatts of output power [1, 2]. It has wide variety of applications in science, industry, civil and military defence. For this growing necessities of generating high power at high frequencies, development of newer type of HPM devices and chronological improvement of the devices are very important. Generally, in BWO, the axially streaming electron beam provides energy to the electromagnetic (EM) wave through resonant, hollow SWS under the application of a strong magnetic field. The SWS slows down the phase velocity of the EM wave for ensuring the exchange of energy between the electron beam and the EM wave through resonant interaction. BWO operates in the negative group velocity region of the dispersion diagram [2-4].

Among the various SWSs like periodic metallic structures, structure filled with plasma or filled with dielectric material etc., metallic SWS has extensive usage due to its sustainability. RF breakdown was the consequence when dielectric disks were introduced periodically in the structure. Thus corrugated metallic structures were employed extensively together with its added advantage of higher power, efficiency and stability [3-5]. Out of different available metallic corrugation profiles, sinusoidally corrugated SWSs (SCSWS) were employed extensively due to its feature of tolerating RF breakdown and high output power. However, researchers explored and proposed some new structures like rectangularly corrugated [6, 7], doubly rippled wall [8], trapezoidally corrugated [9, 10], triangularly corrugated [11], and semi-circular [12, 13] SWSs for higher peak output power and conversion efficiencies and implemented them successfully because of the complexities lied in the fabrication of smooth and precise sinusoidal profile in the inner wall of the SCSWS. Beside these, researchers investigated the possibilities using metamaterials [14] and reported the achievement of dual frequency application [15].

In general, the dispersion relation is determined by applying numerical techniques or performing cold tests. Owing to the restrictions of the (2-D) RF codes for lower pass band modes only and others being structure dependent which requires code modifications for each change in the structure, experimental approach is inevitably necessary for the verification of both the dispersion characteristics and the computational results [16, 17]. Guo *et al.* reported a novel, synthetic technique for the accurate determination of the dispersive characteristics of periodic SCSWS. Any periodic structure having N numbers of periods gives (N+1) discrete resonant frequencies when its ends are appropriately

shorted. This technique is applied for determining the complete dispersion characteristics of both the fundamental and higher order pass band modes for TCSWS. The experimentally measured results are obtained from [10]. Then the results obtained following synthetic technique are compared with the experimental results for TCSWS.

For numerical verification, finite element method (FEM) based high frequency structural simulator (HFSS) and CST microwave studio are used to calculate the electromagnetic field quantities of the SWSs. The cold test using vector network analyzers (VNAs) are usually performed to measure the two port parameters and resonant frequencies of the discrete axial modes. The field variations are measured by perturbation method. From the discrete frequencies of the axial modes, continuous dispersion diagram can be generated. As VNAs in the tens of GHz range are costly equipment real cold test may not be always possible to substantiate the analytical results, high frequency simulators can be used to simulate the cold test and test method can be benchmarked using available experimental results. Here the numerical simulation results are benchmarked so that numerical simulation can be viably used to substantiate the analytical and cold test results and can be used to model different type of SWSs before deploying them to real experiments.

The summarized mathematical relation and description of the numerical verification of dispersion relation for axial modes are presented in section 2. Section 3 presents the comparison between the results obtained following synthetic technique and the experimental results for fundamental as well as higher order modes. Synthesis and comparison of continuous dispersion curve drawn with the simulated and measured discrete frequency values is presented in section 4. It covers the comparison between the numerical simulation results and the analytical results also. Section 5 presents the longitudinal and radial electromagnetic field patterns for axial modes and its comparison with analytically obtained field patterns. Conclusion is presented in section 6.

2. Mathematical Relation and Numerical Verification of Dispersion Relation

The analytical dispersion relation can be obtained by using Rayleigh-Fourier (R-F) method whose rigorous mathematical detail is presented in [9, 10]. A section of the infinitely long axisymmetric cylindrical TCSWS is shown in Fig. 1. Figure 2 depicts the finite length six-period TCSWS cavity with antenna. The size parameters of the SWS are depicted in Table 1. In BWOs, the interaction of wave and beam depend on both the dispersion relation of the SWS and distributions of the EM fields. Studies have been performed for analyzing the EM modes and its interactions with electron beam considering infinite length SWS. Assumption of infinite length is applicable for perfectly matched system where end reflections are not expected.

During real experiments, the finiteness of the SWS has end reflections. The end reflections quantize the EM modes into a number of axial resonant modes. Thus in designing BWO devices, end effects are to be taken into account for analyzing the EM field properties of the axial modes [18].

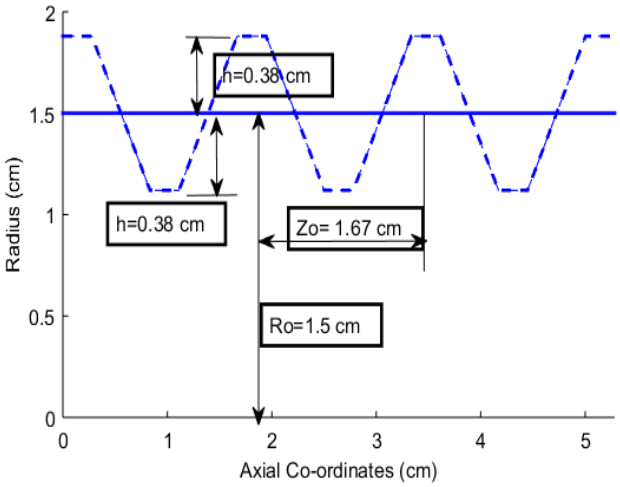

Fig. 1. *Axial profile of the axisymmetric TCSWS*

Table 1 The structure parameters for TCSWS for X-band.

Parameters	$R_o(cm)$	$Z_o(cm)$	$h(cm)$	$K_o(cm^{-1})$
TCSWS	1.50	1.67	0.38	3.76

In order to confirm the analytical and experimental results, the dispersion diagram of the SWS is verified by using professional high frequency full wave simulator like HFSS and CST Microwave studio. The dispersion diagram of

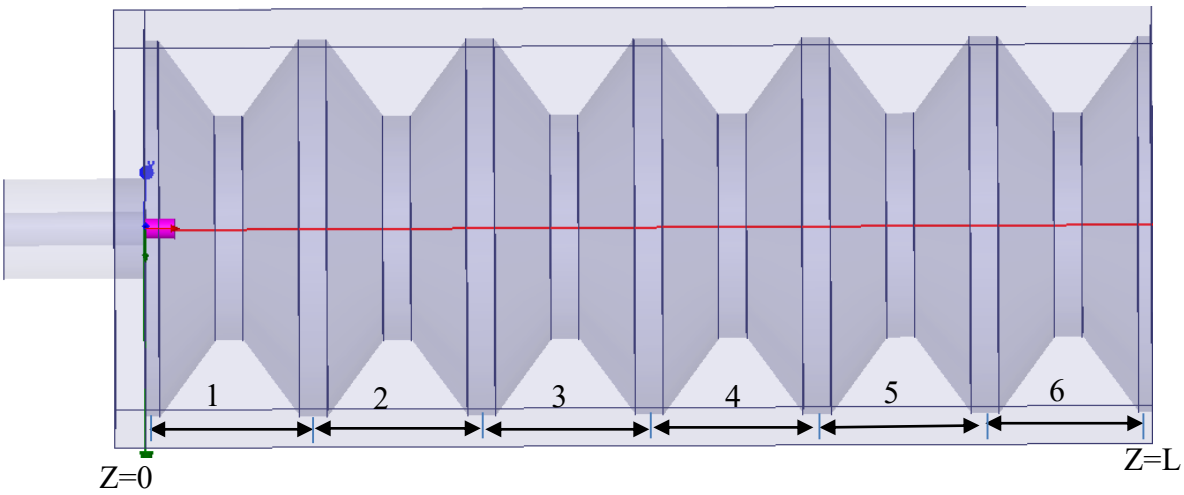

Fig. 2. *3D view of the six-period TCSWS cavity with antenna and shorting plates placed at Z=0 and Z=L*

periodic SWS can be determined numerically in many different ways- namely simulating a Floquet boundary and then calculating the time evolution of the field inside the structure. The Fourier transform of the field will give the frequency information. Alternatively, it can be obtained by using transmission or reflection measurement. In the latter case, continuous dispersion diagram cannot be obtained.

In this work, at first the SWS with trapezoidal corrugation was modelled in HFSS. Six period SWS cavity is prepared by placing shorting plates on its both end faces with a hole for admitting the antenna. A trapezoidally corrugated SWS of finite length with shorting plates placed at Z=0 and Z=L is shown in Fig. 2. Then for numerical simulation in HFSS, boundary conditions namely finite conductivity was assigned. Axial EM modes are excited by a suitable mode launcher (needle type antenna in this case) with the help of wave port assignment in HFSS. Usually the selection of mode launcher is dependent on the degree of coupling between the SWS and the mode launcher. When strong coupling exists between them complete reflection on input side cannot be found. The reflection coefficient on input side becomes small for a disc-type mode launcher [19]. Therefore, needle type antenna is used for measuring the reflections in the SWS cavity [10]. However, one of the major problems in determining the resonant frequency of the axial modes for higher order TM modes is the mode launching due to field perturbation that changes the resonant frequencies of the axial modes at high frequency regime. The other problem can be generation of spurious resonance by imperfect mode excitation [16, 17].

The S-parameters are measured in HFSS by exciting axial modes with the help of needle type antenna as shown in Fig. 3. The S_{11} parameter that corresponds to reflection gives the resonant frequency of the particular mode. With these specific resonant frequencies, the complete dispersion relation can be generated. The frequency of this resonant axial modes lies on the dispersion curve of the corresponding axisymmetric TM mode. The resonant axial modes are spaced in the normalized wavenumber space between 0 to π within the first Brillouin zone of the dispersion diagram. The normalized wavenumber corresponding to axial modes are $0, \pi/6, 2\pi/6, 3\pi/6, 4\pi/6, 5\pi/6, \pi$. The discrete frequency points in the frequency and wavenumber space (f_r, k_r) can be used to synthesize the continuous dispersion relation. This dispersion relation is compared with both the analytical and experimental results. For axisymmetric TM modes the axial electric fields E_z for the SWS can be expressed [18, 19] as

$$E_z(z,r,t) = \sum_{\infty}^{\infty} A_n J_o\left(\frac{\chi_n}{R_o} r\right) e^{i(k_n z - \omega t)} \qquad (1)$$

where J_o is the 0th order Bessel's function of the first kind, $\chi_n^2 = R_o^2(\omega^2/c^2 - k_n^2)$, $k_n = k + nK_0$, k is the axial wavenumber, and n is an integer. For slow spatial harmonic in equation (1) the Bessel's function J_o becomes the modified Bessel's

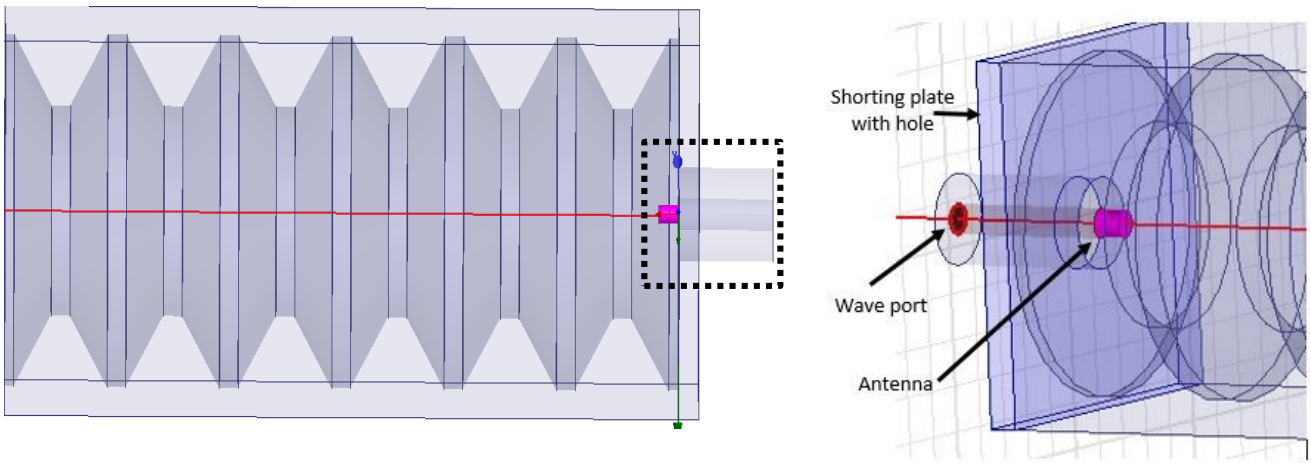

Fig. 3. *Six-period TCSWS cavity with magnified view of antenna for the reflection measurement*

function I_o because of negative χ_n^2. The transverse boundary condition is that the sum of the tangential components of the electric field E_t at the SWS wall is zero. In this case of finite length system with end reflections an additional boundary condition at the ends of the structure must be considered [18-20]. The EM fields in the closed SWS can be expressed as

$$E_z(z,r,t) = e^{-i\omega t}\sum_{n=-\infty}^{\infty} 2A_n J_o\left(\frac{\chi_n}{R_o}r\right)\cos(k_n z) \quad (2)$$

$$E_r(z,r,t) = R_0 e^{-i\omega t}\sum_{n=-\infty}^{\infty} \frac{2A_n k_n}{\chi_n} J_1\left(\frac{\chi_n}{R_o}r\right)\sin(k_n z) \quad (3)$$

$$H_\theta(z,r,t) = -i\varepsilon_0\omega R_0 e^{-i\omega t}\sum_{n=-\infty}^{\infty} \frac{2A_n}{\chi_n} J_1\left(\frac{\chi_n}{R_o}r\right)\cos(k_n z) \quad (4)$$

Equations (2-4) are the standing wave equations for a SWS cavity that results in the formation of resonant axial modes. The relative magnitudes of A_n can be determined by solving the dispersion relation numerically. With a known set of values of A_n, the normalized values of the fields E_z, E_r and H_θ can be calculated from the equations (2-4).

Numerical techniques for this purpose can be a viable alternative for verifying the analytical dispersion relation before performing the real experiment. Following the highly accurate synthetic technique for determination of the dispersion curve, a modular X-band slow wave structure in the form of trapezoidally corrugated metallic waveguide having six periods is modelled. The six period cavity resonated at seven specific frequencies that corresponds to the associated wavenumbers. The resonant reflection peaks of the seven axial modes of the six period cavities associated to the TM_{01} pass band mode is shown in Fig. 4. The reflection profile is achieved by sweeping over the desired frequency range. It is seen that seven resonant peaks have been found in the desired pass band which corresponds to seven resonant axial modes. These discrete resonant frequencies are used to synthesize the continuous curve by using the technique developed earlier for a sinusoidally corrugated SWS [16].

Using the similar setup and mode launcher, reflection profile associated with TM_{02} and TM_{03} are measured by sweeping over the desired frequency range which are shown in Fig. 5 and Fig. 6 respectively. For these two higher order modes, seven peaks are not obtained because of the problems related to mode-launching due to field perturbation. These discrete frequency points for axisymmetric TM modes are used to synthesize the continuous dispersion relation and are compared with both the analytically and experimentally obtained ones.

3. Comparison between the Numerical and Experimental Results

Table 2 shows the comparison between the numerical and experimental results of the resonant frequencies of the axial modes of TCSWS. It can be easily visualized that the numerical results obtained using high frequency structural simulator agree well with their experimental counterparts (Fig. 5 (a), 5 (b) and 5 (c) of [10] respectively) with a maximum deviation of 1.94% for TM_{01} mode, 1.29% for TM_{02} mode and 2.38% for TM_{03} mode.

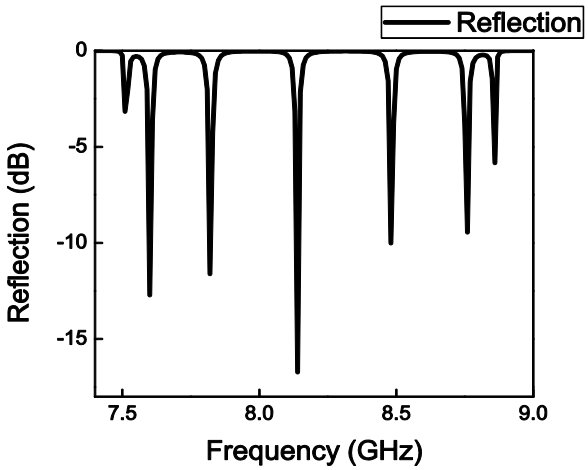

Fig. 4. *Reflection profile of TCSWS for TM_{01} mode*

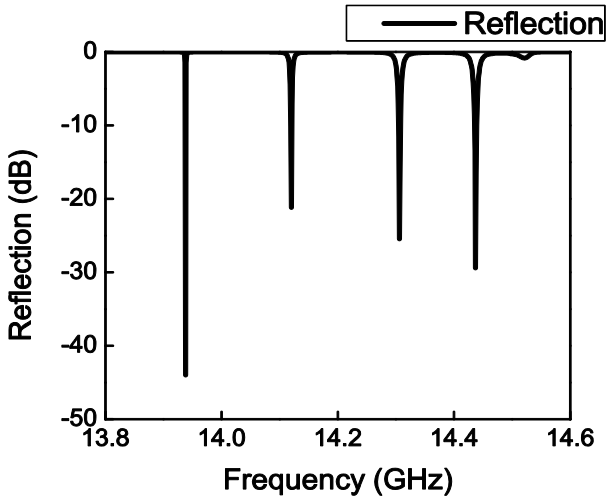

Fig. 5. *Reflection profile of TCSWS forTM_{02} mode*

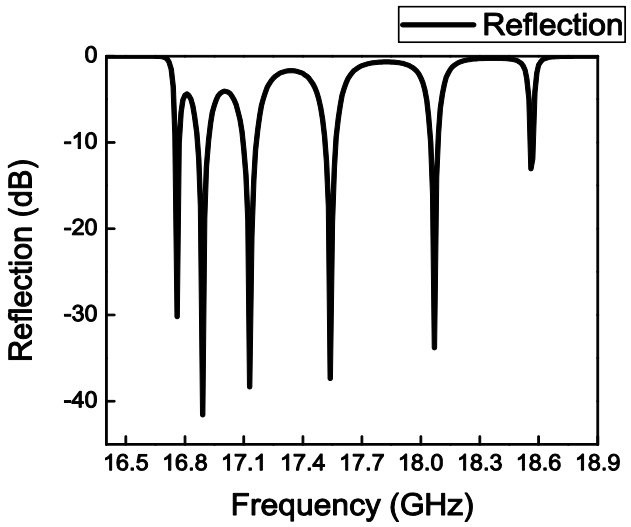

Fig. 6. *Reflection profile of TCSWS for TM_{03} mode*

4. Synthesis of Continuous Dispersion Curves from Numerically Obtained Discrete Frequency Values and Comparison with Analytical Results

The procedure for obtaining complete dispersion relation following synthetic technique using only three and seven terms with excellent accuracy (<1%) is presented in [16]. In principle, for long SWS (large number of periods, N>>1) the complete dispersion relation can be obtained by measuring very large numbers of discrete resonances. The dispersion relation for a periodic SWS using impedance or ABCD matrix of a four terminal network and Floquet theorem is expressed as

$$f = f(\cos kL, G) \qquad (5)$$

where f is the frequency, kL is the phase shift per period and G is SWS dimension related geometric factor. The dispersion relation can be expressed in the form of series:

Table 2 Comparison between simulated and experimental values of the resonant frequency of TM_{01} – TM_{03} modes

Wave number (cm^{-1})	TM_{01}			TM_{02}			TM_{03}		
	HFSS (GHz)	Experimental (GHz)	Deviation (%)	HFSS (GHz)	Experimental (GHz)	Deviation (%)	HFSS (GHz)	Experimental (GHz)	Deviation (%)
0	7.51	7.443	1.947	14.523	14.337	1.297	×	18.802	-----
0.5236	7.60	7.519	1.065	14.473	14.32	1.068	18.567	18.593	0.140
1.0487	7.82	7.745	0.959	14.306	14.264	0.294	18.082	18.017	0.359
1.5708	8.14	8.073	0.823	14.12	14.164	0.310	17.571	17.415	0.887
2.0944	8.48	8.425	0.648	13.938	14.013	0.535	17.274	16.935	1.962
2.618	8.76	8.706	0.616	×	13.869	----	17.054	16.648	2.380
3.1416	8.86	8.826	0.383	×	×	----	16.797	16.552	1.458

$$f = \sum_{m=0}^{\infty} a_m \cos mkL \tag{6}$$

Here a_0, a_1, $a_2 \ldots a_m$ are geometry dependent coefficients which can be determined analytically through numerical calculations or experimental measurement of some specific resonant frequency points for the respective SWS. With these obtained frequencies $f_0, f_1, f_2 \ldots\ldots f_m$, the coefficients can be calculated analytically or numerically by inverting the matrix in equation (7).

$$\begin{bmatrix} f_0 \\ f_1 \\ f_2 \\ - \\ f_m \end{bmatrix} = \begin{bmatrix} \cos 0 & \cos 0 & \cos 0 & - & \cos 0 \\ \cos 0 & \cos\frac{\pi}{m} & \cos\frac{2\pi}{m} & - & \cos\frac{m\pi}{m} \\ \cos 0 & \cos\frac{2\pi}{m} & \cos\frac{4\pi}{m} & - & \cos\frac{2m\pi}{m} \\ - & - & - & - & - \\ \cos 0 & \cos\frac{m\pi}{m} & \cos\frac{2m\pi}{m} & - & \cos m\pi \end{bmatrix} \begin{bmatrix} a_0 \\ a_1 \\ a_2 \\ - \\ a_m \end{bmatrix} \tag{7}$$

Dispersion relation is important for understanding the possible region of interaction between the wave and the electron beam. The knowledge about the probable oscillating frequency and possible operation at positive and/or negative group velocity is obtained from this relation. The complete and continuous dispersion relation has been synthesized and compared for TM_{01} mode of TCSWS with the points obtained from both HFSS simulation and measurement as shown in Fig. 7. The light line ($\omega=kc$) and beam line ($\omega=\beta kc$) with different sets of β are depicted to identify the possible BWO operating point. Qualitative information about the expected oscillation frequency can be obtained from the intersecting point of the beam line and the dispersion curve. BWOs operate at a frequency and wavenumber which can be roughly estimated from the intersecting points. Knowledge about the speed of axial energy transport is gained from the respective group velocity which is basically the derivative of the dispersion characteristics. The analytical dispersion relation is taken from [9,10]. The dispersion curves drawn for TCSWS with the resonant peak values obtained from S_{11} measurement is compared with the dispersion curves drawn with analytical and experimental values. These are shown in Fig. 8, Fig. 9 and Fig. 10 respectively.

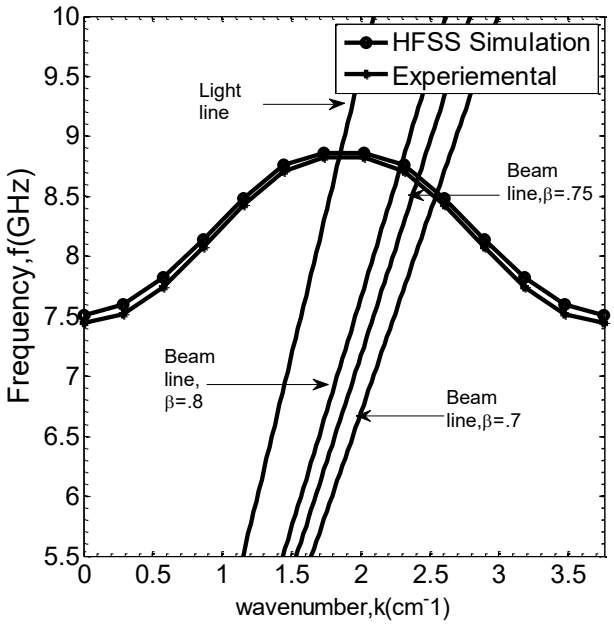

Fig. 7. *The dispersion characteristics of TCSWS for TM_{01} mode.*

The agreements and validations of the simulated results with the analytical and experimental results are evident from the figures. However, the discrepancies are owing to the fact that seven resonant peaks were not obtained for TM_{02} and TM_{03} that led to these deviations.

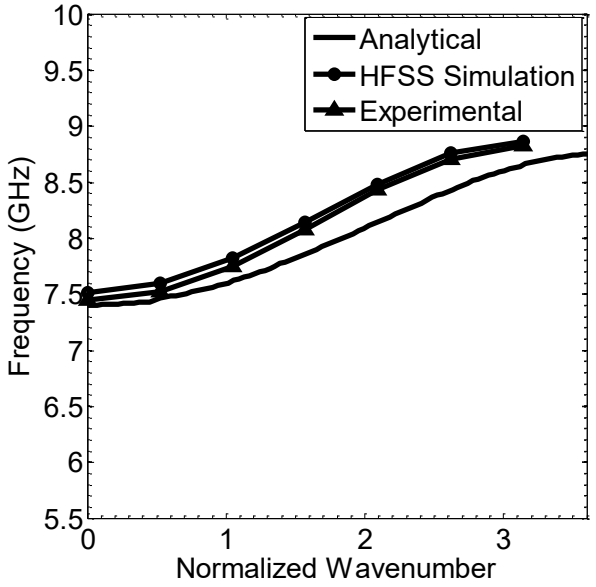

Fig. 8. *Comparison between dispersion curves for TCSWS of TM_{01} mode drawn by using the analytical, simulation and experimental values*

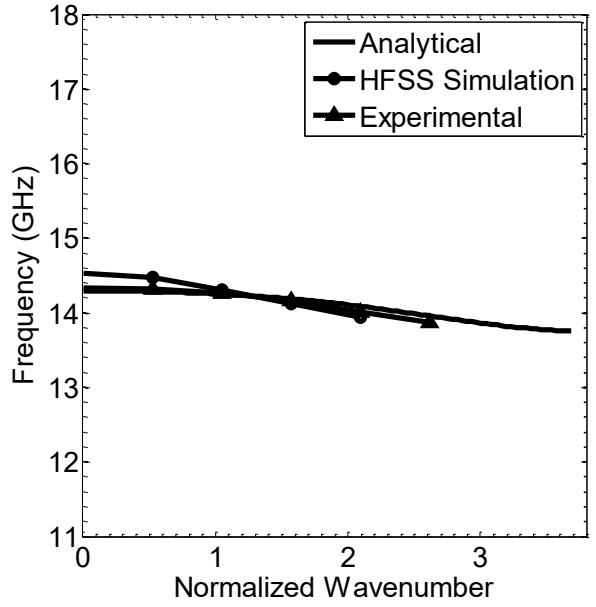

Fig. 9. *Comparison between dispersion curves for TCSWS of TM_{02} mode drawn by using the analytical, simulation and experimental values*

5. Electromagnetic Field Patterns for Axial TM Modes and its Comparison with Analytically Obtained Field Patterns

Examination of the EM field patterns is needed for many reasons, such as to determine the spatial field intensity variation inside the structure for a particular axial mode, to determine the type of the polarization of the EM field (whether TM or TE) inside the waveguide and to determine the energy

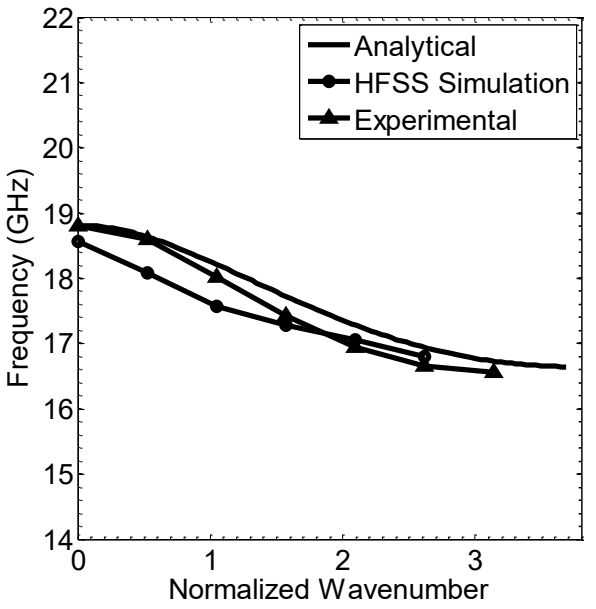

Fig. 10. *Comparison between dispersion curves for TCSWS of TM_{03} mode drawn by using the analytical, simulation and experimental values*

flow through the wave guide. The knowledge about the radius of the electron beam and the vulnerability of the structure for RF breakdown can be gained from the field patterns of the axial modes [4, 21-23]. The electromagnetic field patterns of both longitudinal and radial TM_{01} and TM_{03} modes of TCSWS are calculated using CST microwave studio as shown in Fig. 11 and Fig. 12 respectively. The field distribution is presented using the normalized value of the field strength where red colour indicates the highest value and blue represents the lowest value. The normalized electric field patterns in z direction (x=0, y=0) and normalized electric field patterns along x direction (y=0, z=0) are also depicted in the figures. The density of the field lines represents the strength of the electric field qualitatively. For TM_{01} ($3\pi/6$) mode, the axial pattern of the fields has three zero points and the radial variation of the field has a maximum value on the axis of the structure. For TM_{03} ($3\pi/6$) mode, the axial pattern of the fields has three zero points and the radial variation of the field shifts thrice. The obtained result for TM_{01} mode of TCSWS has been compared with analytically obtained TM_{01} mode of SCSWS from [10] and [21] respectively in Fig. 13. It can be seen that there is no mention worthy difference in the field patterns of the axial modes which shows the agreement and validation of the obtained results.

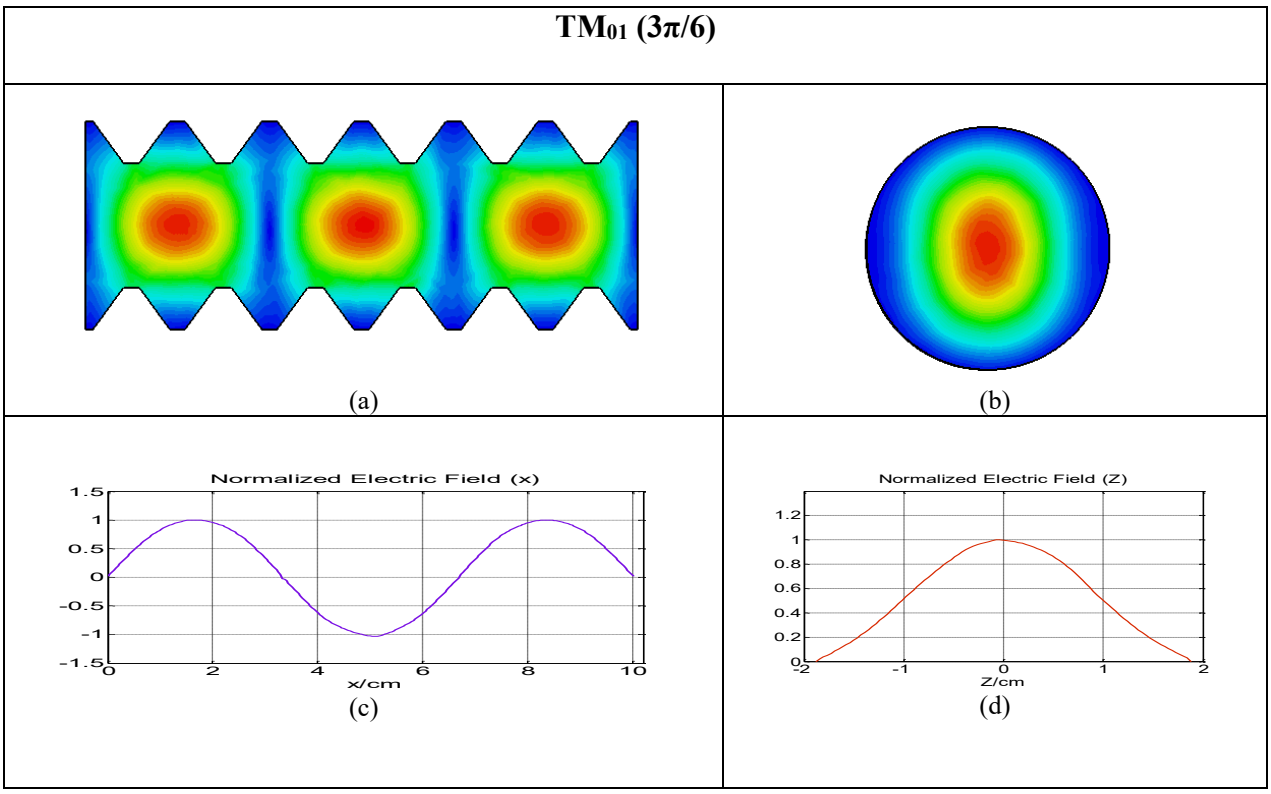

Fig. 11. *Electric field distribution for TM_{01} modes at kzo = 3π/6 of TCSWS. (a) Axial electric field patterns. (b) Radial electric field patterns. (c) Normalized electric field patterns in x direction (y=0, z=0) and (d) Normalized electric field patterns along z direction (x=0, y=0)*

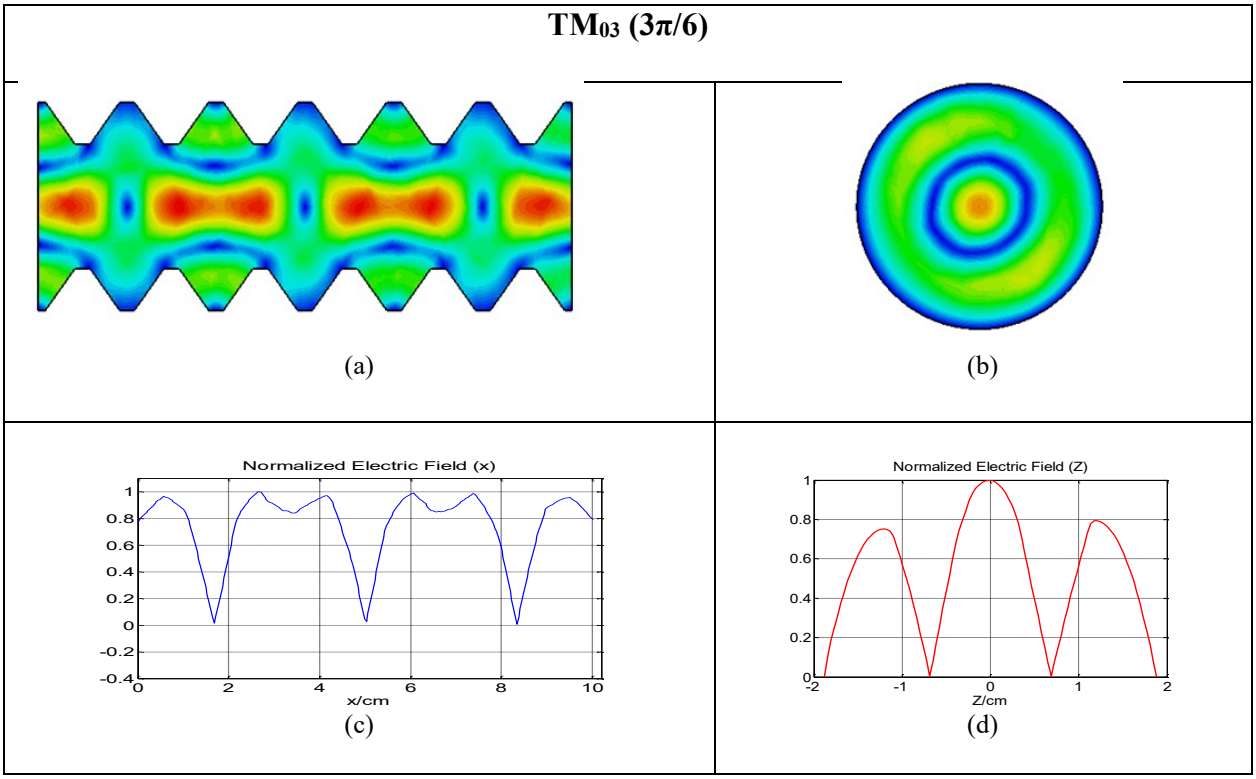

Fig. 12. *Electric field distribution for TM_{03} modes at kzo = 3π/6 of TCSWS. (a) Axial electric field patterns. (b) Radial electric field patterns. (c) Normalized electric field patterns in x direction (y=0, z=0) and (d) Normalized electric field patterns along z direction (x=0, y=0)*

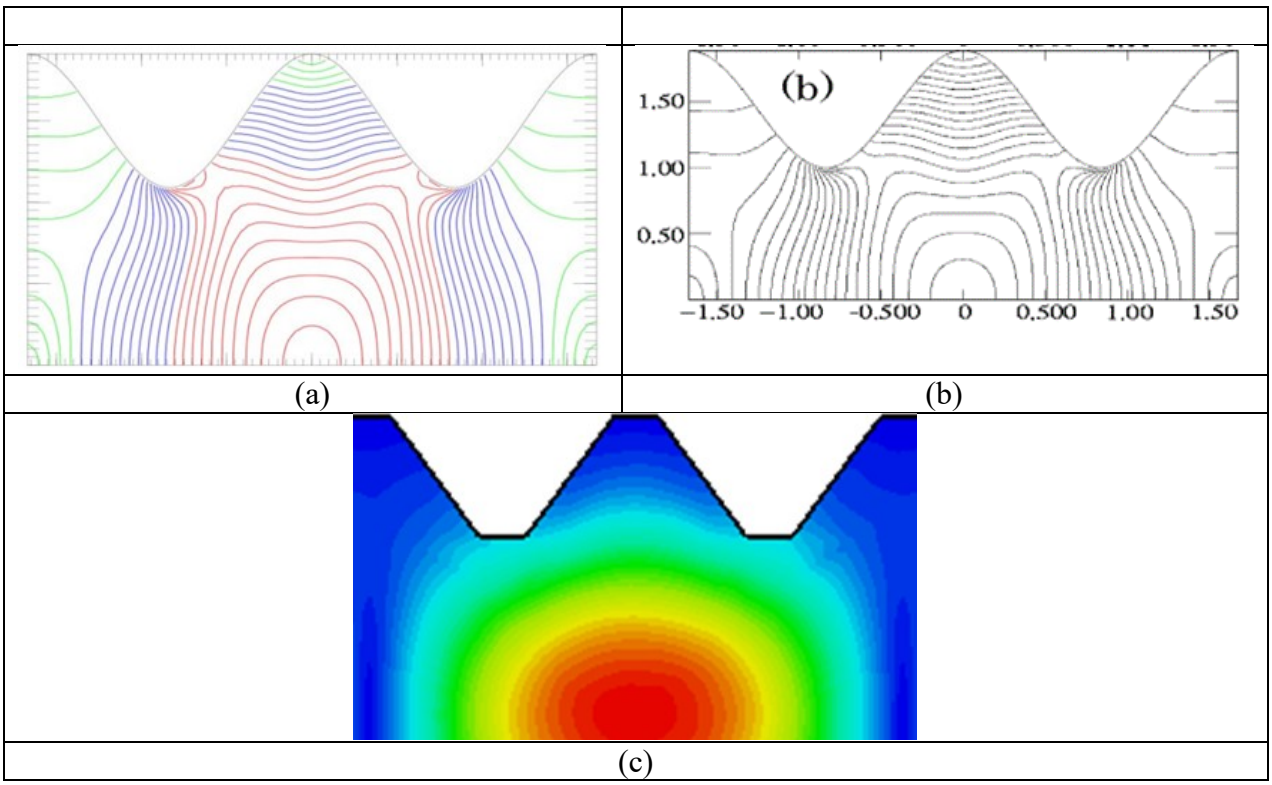

Fig. 13. *Comparison between obtained field patterns and analytical results. (a) Field pattern of TM_{01} mode for SCSWS with kzo =3π/6 [10], (b) Field pattern of TM_{01} mode for SCSWS with kzo =3π/6 [21] (c) Field pattern of TM_{01} mode for TCSWS with kzo =3π/6*

6. Conclusion

The dispersion characteristics and the electromagnetic field properties of fundamental and higher order TM modes of finite length TCSWS cavity having 6 periods are verified in this paper. The complete dispersion curve of the SWS is determined for axial modes from the obtained discrete resonant frequencies following synthetic technique. The dispersion characteristics are compared with both the experimental results and analytical values which show good agreement. The radial and longitudinal field patterns of the axial modes of the SWSs are calculated. The obtained field patterns are compared with analytical patterns that validate the obtained field patterns of the SWSs. Thus, numerical simulation can be used viably to substantiate the analytical and cold test results and can be employed for modelling different type of SWSs before deploying them to real experiments.

7. References

[1] Benford, J., Swegle, A.S., and Schamiloglu, E.: 'High Power Microwaves', (CRC Press, 2007)

[2] Granatstein, V.L., and Alexeff, I.: 'High Power Microwave Sources', (Artech House, Dedham, MA, 1987)

[3] Gaponov-Grekhov, A.V., Granatstein, V. L.: 'Applications of High-power Microwaves', (Artech House, 1994)

[4] Elachi, C.: 'Waves in active and passive periodic structures: A review' Proc. IEEE, 1976, 64, pp. 1666–1698

[5] Gold, S.H. and Nusinovich, G.S.: 'Review of high-power microwave source research', Rev. Sci. Instrum., 1997, 68, (11), pp. 3945–3974

[6] Wang, H., Yang, Z., Zhao, L., et al.: 'Numerical computation of dispersion curves for symmetric and asymmetric modes in an arbitrary cylindrical metal SWS', IEEE Trans. Plasme Sci., 2005, 33, pp. 111–118

[7] Amin, M.R., Ogura, K.: 'Dispersion characteristics of a rectangularly corrugated cylindrical slow-wave structure driven by a non-relativistic annular electron beam', IET Microw. Antennas Propag. 2007, 1, pp. 575–579

[8] Amin, R., Saber, G., Sagor, R.H.: 'Numerical Study of the Dispersion Properties of an X-band Backward Wave

Oscillator with Rectangularly Rippled Wall Resonator', Procedia - Soc. Behav. Sci., 2015, 195, pp. 2548–2555

[9] Amin, M.R., Ogura, K.: 'Temporal Growth Study in Trapezoidally Corrugated Slow-Wave Structure for Backward-Wave Oscillator', IEEE Trans. Plasme Sci., 2013, 41, pp. 2257–2263

[10] Amin, M.R., Ogura, K., Kojima, J., Sagor, R.H.: 'Electromagnetic Properties of a Trapezoidally Corrugated Slow Wave Structure for Backward Wave Oscillators', IEEE Trans. Plasma Sci., 2014, 42, pp. 1495–1501

[11] Saber, M.G., Sagor, R.H., Amin, M.R.: 'Linear analysis of a backward wave oscillator with triangular corrugated slow wave structure', Eur. Phys. J. Plus, 2016, 131, (5), p. 171.

[12] Saber, M.G., Sagor, R.H., Amin, M.R.: 'Numerical study of the dispersion characteristics of a semi-circularly corrugated slow wave structure', Eur. Phys. J. D, 2015, 69, (2), p. 38.

[13] Saber, M.G., Sagor, R.H., Amin, M.R.: 'Temporal growth rate study of a high power backward wave oscillator with semi-circularly corrugated slow wave structure', Eur. Phys. J. Appl. Phys., 2015, 70, (2).

[14] Shiffler, D., Luginsland, J., French, D.M., Watrous, J.: 'A Cerenkov-like Maser Based on a Metamaterial Structure', IEEE Trans. Plasma Sci., 2010, 38, pp. 1462–1465

[15] Song, G., Lin, M., Yu, X., et al.: 'Particle simulation of X-band dual frequency coaxial relativistic backward wave oscillator' 17th Int. Conf. High Power Particle Beams (BEAMS), 2008, pp. 1–4

[16] Guo, H., Carmel, Y., Lou, W.R., et al.: 'A novel highly accurate synthetic technique for determination of the dispersive characteristics in periodic slow wave circuits', IEEE Trans. Microw. Theory Tech.1992, 40, pp. 2086–2094

[17] Wen, G., Li, J., Xiong, X., et al..: 'A novel numerical synthetic technique for determination of the TM_{on} dispersion relation in a coaxial corrugated cylindrical waveguide', Int. J. Infrared Millimetre Waves, 1997, 18, (9), pp. 1713–1724

[19] Amin, M.R., Ogura, K., Kitamura, H., et al.: 'Analysis of the electromagnetic waves in an overmoded finite length slow wave structure', IEEE Trans. Microw. Theory Tech., 1995, 43, pp. 815–822

[20] Ali, M.M., Minami, K., Amano, S., et al.: 'Linear Analysis of a Localized Plasma-Loaded Backward Wave Oscillator Driven by an Annular Intense Relativistic Electron Beam', J. Phys. Soc. Japan, 1991, 60, (8), pp. 2655–2664

[21] Yamazaki, H., Ogura, K., Watanabe, T.: 'Numerical Examination of Electromagnetic Field Properties in a Cylindrical Periodic Slow Wave Structure', J. Plasma Fusion Res. SERIES, 2004 (6), pp. 719–722

[22] W. Main, Y. Cannel, K. Ogura, et al.: 'The electromagnetic properties of open and closed overmoded slow wave resonators for interaction with relativistic electron beams' IEEE Trans. Plasma Sci., 1994, 22, (2), pp. 566-577.

[23] Amin, M.R., Ogura, K., et al 'Electromagnetic Field Properties of Axial Modes in a Finite Length X-Band Slow Wave Structure', J. Phys. Soc. Japan, 1996, 65, (2), pp. 627–634